The Journal of Physical Chemistry

 VOLUME 99, NUMBER 13, MARCH 30, 1995

LETTERS

Full Configuration Interaction Molecular Dynamics of Na_2 and Na_3

Zhihua Liu,† Lawrence E. Carter, and Emily A. Carter*

Department of Chemistry and Biochemistry, University of California, Los Angeles, California 90095-1569

Received: December 20, 1994®

We extend our *ab initio* molecular dynamics methods to more exact wave functions, including complete active space multiconfiguration self-consistent-field (CASSCF) and full configuration interaction (full CI) wave functions. These extensions are critical for describing properly the dynamics of bond formation/dissociation and isomerization, as we illustrate here by examining the bond dissociation/formation of Na_2 and the isomerization ("pseudorotation") of Na_3 with full CI dynamics. Equivalencing of all three atoms of Na_3 is found to proceed *first* via facile inversions through linear structures, which occur more often than conventional pseudorotation (via obtuse to acute to obtuse isosceles triangles).

Introduction

Since the introduction by Car and Parrinello of an extended Lagrangian scheme for integrating the classical equations of motion for nuclei subject to quantum mechanical forces due to the associated electrons,[1] the field of *ab initio* molecular dynamics (AIMD) has generated widespread interest. Its appeal stems from the ability to carry out classical dynamics on an *ab initio* potential energy surface (PES), without having to precalculate the surface and fit it to an analytic function whose form might bias the dynamics observed. Car and Parrinello achieved this within the framework of a fictitious dynamics for a density functional theory (DFT) description of the electrons that was updated as the nuclei moved. In the DFT-MD realm, advances to and variations on the original algorithm include the more exact Born−Oppenheimer dynamics,[2] extensions to other ensembles,[3] the faster orbital-free DFT dynamics,[4] inclusion of nonlocal corrections to DFT,[5] and faster multiple time step methods for AIMD.[6] In parallel with these developments have been AIMD algorithms based on molecular quantum mechanical wave functions, including work on restricted Hartree−Fock (RHF), restricted open-shell HF (ROHF), and generalized valence bond (GVB) MD.[7,8] Extensions to or variations of these methods include faster AIMD multiple time step algorithms,[9] propagation of the orbital rotation matrix to avoid implementing orthonormalization constraints,[10] and implementation of a new wave function convergence acceleration method coupled with Born−Oppenheimer MD.[11] Finally, a related approach used analytic first and second energy derivatives to construct a locally quadratic approximation to HF PES's, which then were used to integrate classical trajectories for small polyatomic molecules.[12]

Our previous work focused on the development of and improvements to algorithms for HF- and GVB-based MD.[8,9,11] However, for many situations, it is not sufficient to describe the forces on the nuclei with wave functions that either do not include correlation (HF) or include it only at a low level (GVB). In particular, HF is notoriously inaccurate for describing bond breaking properly, and while GVB ameliorates this problem somewhat, it still involves solving for the lowest energy valence-bond-type resonance structure at each geometry. The problem with this is that while GVB is useful at the end points (equilibrium geometries or dissociated fragments), at points in between, for example at saddle points, it falls short of a reasonable description because such areas on potential energy surfaces really should involve a linear combination of several or many valence bond resonance structures. As a result, studying the isomerization of clusters[13] or the breaking and

† Present address: Joint Research Center for Atom Technology (JRCAT), 1-1-4 Higashi, Tsukuba, Ibaraki 305, Japan.

® Abstract published in *Advance ACS Abstracts,* March 15, 1995.

0022-3654/95/2099-4355$09.00/0

making of chemical bonds in a chemical reaction often may not be portrayed accurately by a GVB-MD calculation. This provided the motivation for the current work, in which we extend our AIMD methods to wave functions that indeed not only include higher (or full) levels of electron correlation to improve the accuracy of the PES but also make sure to include all possible valence resonance structures important in isomerization and bond breaking/making processes. Obviously full CI wave functions provide such a description, since they are exact within the basis set that is used, while CASSCF wave functions ensure inclusion of all possible valence electron configurations (resonance structures).[14]

Herein we apply our full CI dynamics method to bond breaking/forming in Na_2 and the isomerization of Na_3. These two simple cases serve to illustrate how smoothly the dynamics behave once the wave function is complete and further how our technique can overcome problems observed earlier in DFT-MD studies of the same systems.[15] In particular, DFT exhibited unphysical behavior as bonds were broken, leading to large increases in the fictitious kinetic energies that represent changes in the Kohn–Sham orbital coefficients with time. The reason for the unphysical behavior is simple to understand: large changes in the shapes of the bond orbitals must occur during dissociation and re-formation, and the local density approximation to DFT, like restricted HF, has difficulty in describing those changes because it must convert one doubly-occupied orbital into two singly-occupied orbitals upon dissociation. The large increases in the fictitious kinetic energies resulted in nonconserved dynamics due to energy being drained away from the real system and into the fictitious system. This problem was solved approximately by coupling independent thermostats to the up spin and down spin orbital dynamics.[15] We will see that our method retains conserved dynamics throughout all stages of bond dissociation and formation, without resorting to thermostating procedures.

Theoretical Method

We wrote a classical microcanonical (constant number of particles, volume, and energy) molecular dynamics code that interfaces to either of two conventional molecular electronic structure packages, GAMESS[16] and HONDO,[17] which supply the full CI (FCI) or CASSCF energies and forces to the MD code. We have found that HONDO is more efficient than GAMESS under many circumstances; however, the results presented here were performed primarily using GAMESS. The current version of our AIMD code uses HONDO exclusively. Our MD code utilizes the velocity Verlet integrator[18] to integrate the classical equations of motion for the nuclei subject to the full quantum mechanical forces, $F_i = -\nabla_i\langle\Psi|H|\Psi\rangle$. The wave function is updated at each time step not by fictitious propagation of the coefficients as in the Car–Parrinello (C–P) method but by Born–Oppenheimer dynamics in which the wave function is reoptimized at each time step to stay on the Born–Oppenheimer surface. We have found that for small systems such Born–Oppenheimer dynamics, when combined with more robust wave function convergence methods, allows one to use a significantly longer time step than any C–P method we developed previously, and hence it becomes more efficient to use Born–Oppenheimer dynamics in the context of HF-MD, GVB-MD, CASSCF-MD, or FCI-MD.[11b]

For the Na cluster test cases described here, we used the same effective core potential and basis set for Na as in our previous HF- and GVB-MD work,[8,9] which consists of a double-zeta plus double-polarization basis set representing each valence s-electron.[19] The full CI calculations for Na_2 and Na_3 utilized 136 and 4600 configuration state functions, respectively, which correspond respectively to two electrons distributed all possible ways in 16 orbitals spin-coupled into a singlet state and three electrons distributed all possible ways in 24 orbitals spin-coupled into a doublet state. We found for Na_2 that we could use time steps as large as 500 au (≅12 fs) without suffering any loss of energy conservation. For Na_3, we were more conservative, utilizing time steps of 150 au for trajectories with characteristic temperatures up to 600 K and 50 au for trajectories with characteristic temperatures higher than that. The trajectories for Na_2 were up to 12 ps in length, while the trajectories for Na_3 ranged from 2.4 to 24 ps, depending on the temperature. Atomic units were used throughout, where the mass of Na atom is 22.9898 amu = 41 409.3 au and 1 fs = 41.32 au.

Results and Discussion

Na_2. Laser-induced fluorescence experiments by several groups[20] have converged on a dissociation energy of D_e = 6022.6 ± 1.0 cm^{-1}, a vibrational frequency of ω_e = 159.1 cm^{-1}, and an equilibrium bond length of R_e = 5.82 bohrs for the ground state of Na_2. The highest quality *ab initio* electronic structure prediction available, an effective core potential two-electron full CI calculation in a much larger basis set than we have employed (108 basis functions up through $l = 3$ in angular momentum), yields D_e = 5892 cm^{-1}, ω_e = 159.1 cm^{-1}, and R_e = 5.83 bohrs for the $^1\Sigma_g^+$ ground state.[21] The excellent agreement between theory and experiment shows that the frozen core approximation is not a serious one; however, it appears that a much larger basis than we can afford to use in dynamics at present is necessary to achieve quantitative accuracy. Indeed, a full CI within our much smaller basis set (16 versus 108 functions) yields D_e = 3697 cm^{-1}, ω_e = 136 cm^{-1}, and R_e = 6.31 bohrs. Thus, the frequency and bond length are only off by 14% and 8%, respectively, but the well depth is off by 37%. These error bounds tell us that the curvature and location of minima on our PES upon which we are doing dynamics are expected to be reasonable; however, the well depths are too shallow. We therefore will consider primarily qualitative features in the dynamics presented here.

Figure 1 displays the dynamical behavior of two Na atoms which start to approach one another from 16 bohrs apart and zero initial velocity. The attractive force pushes the atoms together to form a bond. At the bottom of the potential well, their maximum velocity is achieved, and then the kinetic energy of course pushes the two atoms even closer, up the repulsive wall, until the energy is completely transformed again into potential energy and the nuclei become stationary again at their nearest approach point. Then, the repulsive force pushes the nuclei apart until the atoms return to their original starting point with zero velocity. Figure 1a shows that the total energy of the system (nuclear kinetic plus potential energy, the latter of which is the full CI total energy) is conserved over 500 000 au (≅12 ps), with no sign of drift whatsoever. The regular beat pattern seen is indicative of unchanging dynamics, where the time between beats corresponds to one complete period of oscillation of the two Na atoms. The energy fluctuations are merely due to the fact that the nuclei are moving much faster in the attractive part of the potential well, and the energy is fluctuating because of the fact we are using a constant integration time step when in fact it would be preferable to use a shorter time step in this region of the potential where the nuclei move fastest. This is amply illustrated in Figure 1b,c, where we see a blowup of one such beat in the total energy in Figure 1b and the corresponding large changes in potential energy (Figure 1c), which look precisely as one would expect for two

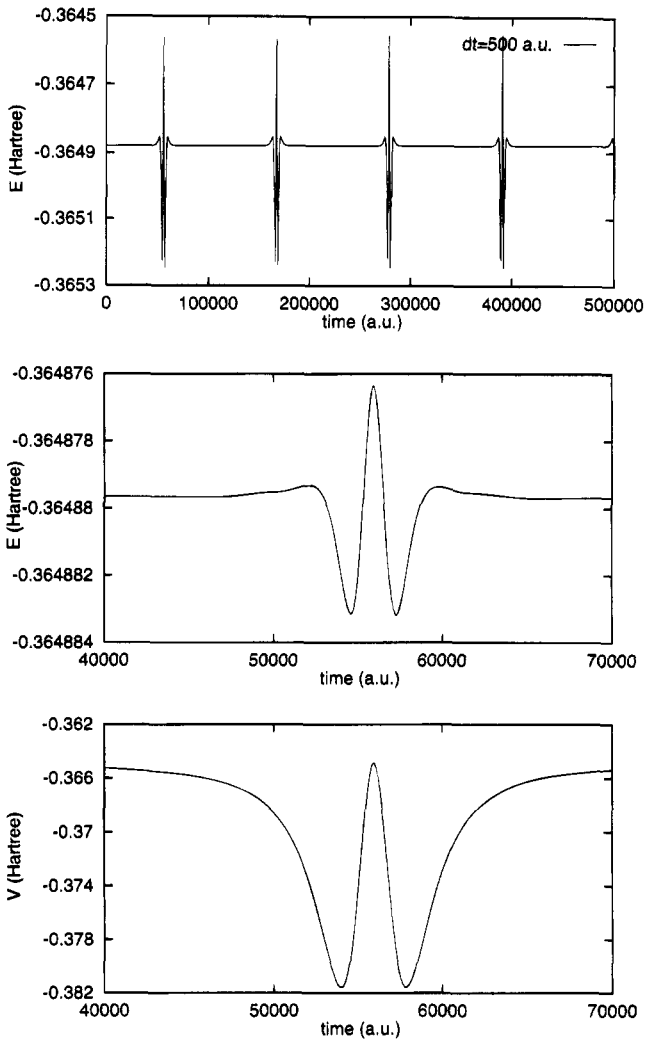

Figure 1. (a, top) Total energy (hartrees) versus time (au) of two Na atoms first forming a bond and then breaking it, over and over again, during a period of ≅12 ps. Total energy = nuclear kinetic energy + full CI total energy. (b, middle) Blowup of one beat in the total energy versus time. (c, bottom) Corresponding behavior of full CI total energy (*i.e*, nuclear potential energy) over the same time period.

Na atoms coming together and then dissociating (similar to two Morse potentials placed back to back). Thus the beats are to be expected, and we emphasize that the overall energy conservation is excellent, unlike the situation with DFT-MD described earlier. We conclude that full CI dynamics can treat bond dissociation in a realistic manner.

Na_3. ESR spectra of Na_3 indicate that below 20 K the structure is static and corresponds to a $^2B_2$ obtuse isosceles triangle, while above 20 K the structure is fluxional, with all three Na atoms becoming equivalent on the ESR time scale ($\leq 10^{-8}$ s).[22] Resonant two-photon ionization (TPI) and stimulated emission pumping (SEP) spectra revealed the normal modes of the ground state of Na_3, assigned as $\omega_{bend} = 50$ cm^{-1}, $\omega_{asym\ str} = 87$ cm^{-1}, and $\omega_{sym\ str} = 135-140$ cm^{-1}.[23] Optical double-resonance spectroscopy (ODR) was used to extract the structure of the ground $^2B_2$ state of Na_3: an obtuse isosceles triangle with an apex angle of 79.69 ± 0.23° and an apex to terminal atom bond length of 3.244 ± 0.006 Å.[24]

The extremely flat potential energy surface of Na_3 has been studied extensively theoretically, from an *ab initio* electronic structure viewpoint,[25-27] a path integral Monte Carlo approach,[28] and a classical dynamical one.[29-31] Multireference CI and DFT calculations[25-27] found a global minimum of $^2B_2$ symmetry (obtuse isosceles triangle) with normal modes of 84−86, 89,

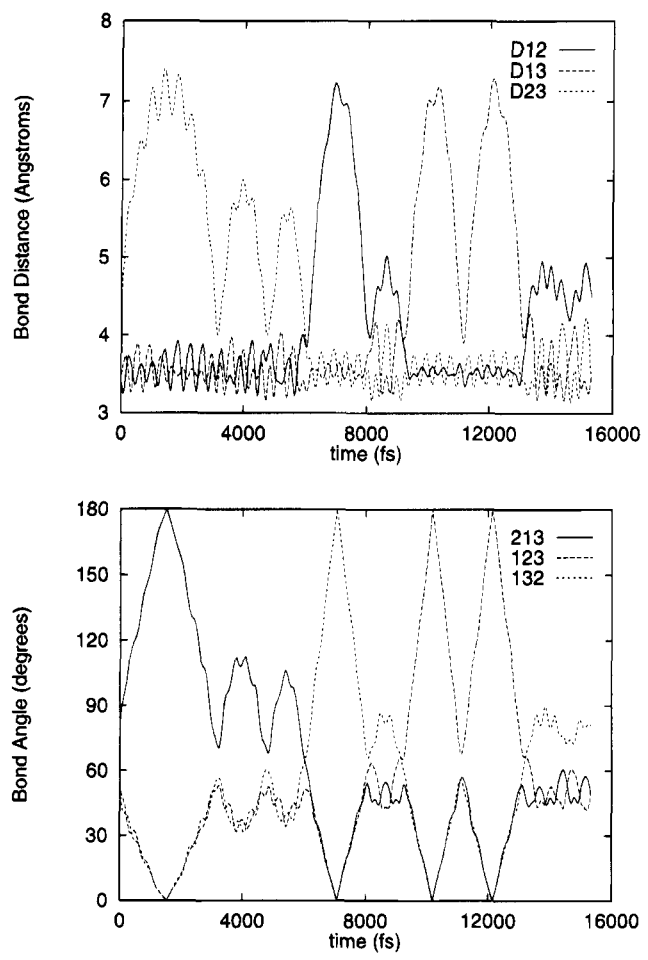

Figure 2. (a, top) Na−Na bond distances (Å) and (b, bottom) bond angles (deg) versus time (fs) for Na_3 at $\langle T \rangle = 137 \pm 7$ K.

and 135−147 cm^{-1},[25,27] $^2A_1$ acute isosceles triangle and $^2\Sigma_u^+$ linear saddle points respectively 131−323 and 484−1045 cm^{-1} higher,[25-27] and a conical intersection at the equilateral triangle structure ($^2E'$) located 560−669 cm^{-1} above the global minimum.[25,27] Our full CI calculations predict roughly the same ordering of critical points, with a $^2B_2$ global minimum [R_e(apex−terminal atom) = 3.49 Å, θ_e(apex) = 79.1°], a $^2A_1$ saddle point [R_e(apex−terminal) = 4.03 Å, θ_e = 48.5°] 148 cm^{-1} higher, and a $^2\Sigma_u^+$ linear saddle point [R_e(apex−terminal) = 3.57 Å] 174 cm^{-1} above the minimum, with the $^2E'$ equilateral triangle (R_e = 3.68 Å) conical intersection lying 743 cm^{-1} above the equilibrium structure. Thus, we expect that finite temperature dynamics up to ≅1000 K on our full CI surface should allow easy access to isomerization without passing through the conical intersection. This allows us to consider classical dynamics without concern for nonadiabatic effects or issues of quantum phase relationships. Indeed, previous classical mechanical studies of Na_3 dynamics[29,30] on an *ab initio*-derived potential surface[32] showed that classical dynamics captures the essential dynamical features below, at, and even above the conical intersection. We now discuss our results of full CI dynamics of Na_3.

We carried out Na_3 trajectories starting from an arbitrary obtuse (>60°) isosceles triangle (apex angle = 80.0° and apex−terminal atom bond lengths = 3.485 Å) and random in-plane velocities (with translational and rotational motion removed) chosen from a Boltzmann distribution at 300, 600, and 1000 K, respectively. This yielded average temperatures over the length of each trajectory of 137 ± 7, 342 ± 17, and 710 ± 32 K, respectively. Figures 2 and 3 display the internal coordinates (bond lengths and bond angles) versus time for the lowest and

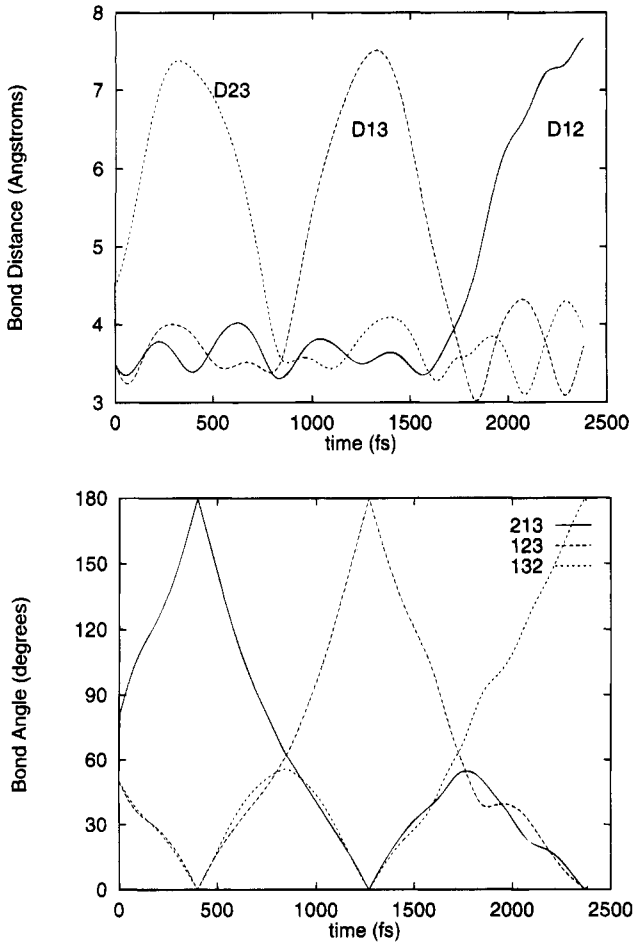

Figure 3. (a, top) Na−Na bond distances (Å) and (b, bottom) bond angles (deg) versus time (fs) for Na_3 at $\langle T \rangle = 710 \pm 32$ K.

highest temperature cases. In Figures 2a and 3a we see that, over the course of the trajectories, two bond lengths stay short, and one on average is longer but undergoes some oscillatory motion; these clearly correspond to obtuse isosceles triangle configurations. The interesting features occur at ≅6, 9, and 13 ps for the 137 K case and at ≅0.8 and 1.7 ps for the 710 K case; at these points, the identity of the long bond switches, indicating that an isomerization has taken place. Not surprisingly, the pseudorotation occurs more frequently at higher temperatures. Even more instructive, however, is to examine Figures 2b and 3b, which depict the time evolution of the bond angles in Na_3 at the two different temperatures. We see that the angles tend to oscillate around those expected for obtuse isosceles triangles (two angles <60° and one >60°). Note that the equilateral triangle conical intersection is never traversed, confirming that nonadiabatic effects at these temperatures are not important. We learn something further from these plots: the cluster can easily access a linear structure, at earlier times and more frequently than isomerization occurs. Linearization occurs at ≅1.5, 7, 10, and 12 ps in the 137 K case and at ≅0.4, 1.3, and 2.4 ps in the 710 K case. Examination of trajectory movies indicates that each of the linearization events results in inversion of the cluster through the middle Na atom. We know that the inversion barrier is probably too small at the small basis full CI level, and this may affect the frequency of these inversion events; however, they still should occur at, *e.g.*, room temperature. Thus, we conclude that *dynamical inversion on the very flat potential surface of Na_3 is competitive with pseudorotation.*

Finally, we have calculated power spectra for Na_3 for the low-temperature case (137 ± 7 K) in order to compare with the known fundamental frequencies of Na_3 observed via the

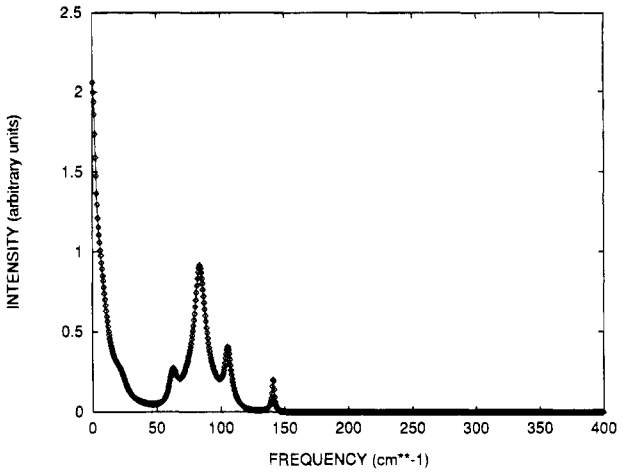

Figure 4. Vibrational (power) spectrum in cm^{-1} for Na_3 at $\langle T \rangle = 137 \pm 7$ K.

TPI and SEP experiments of Broyer *et al.*[23] In order to improve the quality of the statistics, we first followed the trajectory out to ≅24 ps. Then the velocity autocorrelation function, $\langle \mathbf{v}(0) \cdot \mathbf{v}(t) \rangle$, was computed for each atom in Na_3, and these results were then averaged. We then calculated power spectra using two different algorithms: fast Fourier transform (FFT) and maximum entropy (ME) techniques.[33] By varying the number of k points in the FFT and the number of poles in the ME, we were able to establish fairly conclusively which peaks in the spectrum were noise and which were real. Shown in Figure 4 is an example of a ME spectrum, computed with 300 poles using 5000 data points from the velocity autocorrelation function. We see the presence of four peaks at 63, 83.5, 105, and 141 cm^{-1}. The peaks most independent of the number of poles (the one input parameter in the ME method) were the peaks at 83.5 and 141 cm^{-1}. Broyer *et al.* assigned the lowest frequencies observed in their SEP spectrum to the bending vibration at $\nu_2 = 50$ cm^{-1}, the asymmetric stretch at $\nu_3 = 87$ cm^{-1}, the first overtone of the bend at $2\nu_2 = 96$ cm^{-1}, and the symmetric stretch at $\nu_1 = 135-140$ cm^{-1}. Thus, we find very good agreement with experiment for the symmetric and asymmetric stretching modes (within 3.5 cm^{-1}), which indeed are the two modes we are most confident in assigning as real, given that they invariably appear in all spectra we computed. The modes at 63 and 105 cm^{-1} grow in as the number of poles in the ME method grows, and these shift by up to ≅10 cm^{-1} down in energy in the FFT approach depending on the number of k points; thus, we are less confident in our assignment of these modes as the bending and bending overtone vibrations. They may be these modes, but the error bars on the values are at least 10 cm^{-1}. However, even given these errors, we see that the agreement between theory and experiment is rather good. Note finally that while the peak positions are expected to be trustworthy, the intensities derived from these techniques are not particularly meaningful quantities, as they obey no dipole selection rules.

Conclusions

We have shown that using forces on nuclei derived from *ab initio* full CI wave functions now allow one to realistically describe bond-breaking and isomerization pathways in chemical dynamics, including fairly accurate prediction of vibrational spectra. We have demonstrated that this technique does *not* suffer from the nonadiabaticity problems encountered using DFT-MD, namely, nonconservation of energy via energy transfer from real to fictitious degrees of freedom. For the specific case of Na_3, we have suggested that, for temperatures

above 100 K, inversion of the obtuse isosceles triangular equilibrium structure through a linear configuration is facile on the time scale of pseudorotation and thus should be considered in future analysis of the dynamics of the alkali triatomics. For larger molecules, it is clear that full CI methods will be prohibitively expensive, and therefore forces derived from CASSCF wave functions should provide adequate descriptions of such dynamical processes, as they contain all possible valence resonance structures that will be important in the bond breaking and forming that occurs in chemical reactions. We are pursuing currently such approaches to studying the dynamics of bimolecular reactions.[34]

Acknowledgment. We are grateful to the Office of Naval Research for primary support of this work. E.A.C. also acknowledges support from the National Science Foundation, the Camille and Henry Dreyfus Foundation, and the Alfred P. Sloan Foundation via Presidential Young Investigator, Teacher–Scholar, and Research Fellow Awards, respectively. We would also like to thank Prof. Mark Gordon and Dr. Mike Schmidt for supplying us with a copy of the GAMESS electronic structure code and Dr. Michel Dupuis for discussions about HONDO.

References and Notes

(1) Car, R.; Parrinello, M. *Phys. Rev. Lett.* **1985**, *55*, 2471.
(2) See, for example: Barnett, R. N.; Landman, U.; Nitzan, A.; Rajagopal, A. *J. Chem. Phys.* **1991**, *94*, 608. Wentzcovitch, R. M.; Martins, J. L. *Solid State Commun.* **1991**, *78*, 831. Barnett, R. N.; Landman, U. *Phys. Rev. B* **1993**, *48*, 2081.
(3) (a) Stich, I.; Car, R.; Parrinello, M. *Phys. Rev. Lett.* **1989**, *63*, 2240. (b) Buda, F.; Car, R.; Parrinello, M. *Phys. Rev. B* **1990**, *41*, 1680. (c) Wentzcovitch, R. M.; Martins, J. L.; Price, G. D. *Phys. Rev. Lett.* **1993**, *70*, 3947.
(4) (a) Pearson, M.; Smargiassi, E.; Madden, P. A. *J. Phys.: Condens. Matter* **1993**, *5*, 3221. (b) Smargiassi, E.; Madden, P. A. *Phys. Rev. B* **1994**, *49*, 5220.
(5) Laasonen, K.; Parrinello, M.; Car, R.; Lee, C.; Vanderbilt, D. *Chem. Phys. Lett.* **1993**, *207*, 208.
(6) Tuckerman, M. E.; Parrinello, M. *J. Chem. Phys.* **1994**, *101*, 1316.
(7) Field, M. *J. Phys. Chem.* **1991**, *95*, 5104.
(8) (a) Hartke, B.; Carter, E. A. *Chem. Phys. Lett.* **1992**, *189*, 358. (b) Hartke, B.; Carter, E. A. *J. Chem. Phys.* **1992**, *97*, 6569.
(9) (a) Hartke, B.; Gibson, D. A.; Carter, E. A. *Int. J. Quantum Chem.* **1993**, *45*, 59. (b) Gibson, D. A.; Carter, E. A. *J. Phys. Chem.* **1993**, *97*, 13429.
(10) Willetts, A.; Handy, N. C. *Chem. Phys. Lett.* **1994**, *227*, 194.
(11) (a) Ionova, I. V.; Carter, E. A. *J. Chem. Phys.* **1995**, *102*, 1251. (b) Gibson, D. A.; Ionova, I. V.; Carter, E. A. *Chem. Phys. Lett.*, submitted.
(12) (a) Helgaker, T.; Uggerud, E.; Jensen, H. J. A. *Chem. Phys. Lett.* **1990**, *173*, 145. (b) Helgaker, T.; Uggerud, E. *J. Am. Chem. Soc.* **1992**, *114*, 4265. (c) Chen, W.; Hase, W. L.; Schlegel, H. B. *Chem. Phys. Lett.* **1994**, *228*, 436.
(13) Hartke, B.; Carter, E. A. *Chem. Phys. Lett.* **1993**, *216*, 324.
(14) Roos, B. O. *Adv. Chem. Phys.* **1987**, *69*, 399.
(15) Fois, E. S.; Penman, J. I.; Madden, P. A. *J. Chem. Phys.* **1993**, *98*, 6361.
(16) Schmidt, M. W.; Baldridge, K. K.; Boatz, J. A.; Elbert, S. T.; Gordon, M. S.; Jensen, J. H.; Koseki, S.; Matsunaga, N.; Nguyen, K. A.; Su, S.; Windus, T. L.; Dupuis, M.; Montgomery, Jr., J. A. *J. Comput. Chem.* **1993**, *14*, 1347.
(17) Dupuis, M.; Marquez, A.; Chin, S. *HONDO 8.4 from Chem-Station*, IBM Corp., Neighborhood Road, Kingston, NY, 1993.
(18) Swope, W. C.; Andersen, H. C.; Berens, P. H.; Wilson, K. R. *J. Chem. Phys.* **1982**, *76*, 637.
(19) Melius, C.; Goddard, W. A. III *Phys. Rev. A* **1974**, *10*, 1528.
(20) (a) Kato, H.; Matsui, T.; Noda, C. *J. Chem. Phys.* **1982**, *76*, 5678. (b) Verma, K. K.; Bahns, J. T.; Rajaei-Rizi, A. R.; Stwalley, W. C.; Zemke, W. T. *J. Chem. Phys.* **1983**, *78*, 3599. (c) Barrow, R. F.; Verges, J.; Effantin, C.; Hussein, K.; D'Incan, J. *Chem. Phys. Lett.* **1984**, *104*, 179. (d) Babaky, O.; Hussein, K. *Can. J. Phys.* **1989**, *67*, 912.
(21) Magnier, S.; Millie, Ph.; Dulieu, O.; Masnou-Seeuws, F. *J. Chem. Phys.* **1993**, *98*, 7113.
(22) (a) Lindsay, D. M.; Herschbach, D. R.; Kwiram, A. L. *Mol. Phys.* **1976**, *32*, 1199. (b) Lindsay, D. M.; Thompson, G. A. *J. Chem. Phys.* **1982**, *77*, 1114.
(23) (a) Broyer, M.; Delacretaz, G.; Labastie, P.; Wolf, J.-P.; Wöste, L. *J. Phys. Chem.* **1987**, *91*, 2626. (b) Broyer, M.; Delacretaz, G.; Ni, G.-Q.; Whetten, R. L.; Wolf, J.-P.; Wöste, L. *Phys. Rev. Lett.* **1989**, *62*, 2100.
(24) Eckel, H.-A.; Gress, J.-M.; Biele, J.; Demtröder, W. *J. Chem. Phys.* **1993**, *98*, 135.
(25) Martin, R. L.; Davidson, E. R. *Mol. Phys.* **1978**, *35*, 1713.
(26) Martins, J. L.; Car, R.; Buttet, J. *J. Chem. Phys.* **1983**, *78*, 5646.
(27) Cocchini, F.; Upton, T. H.; Andreoni, W. *J. Chem. Phys.* **1988**, *88*, 6068.
(28) Hall, R. W. *Chem. Phys. Lett.* **1989**, *160*, 520.
(29) Gomez Llorente, J. M.; Taylor, H. S.; Pollak, E. *Phys. Rev. Lett.* **1989**, *62*, 2096.
(30) Gomez Llorente, J. M.; Taylor, H. S. *J. Chem. Phys.* **1989**, *91*, 953.
(31) Morais, V. M. F.; Varandas, A. J. C. *J. Phys. Chem.* **1992**, *96*, 5704.
(32) Thompson, T. C.; Izmirlian, Jr., G.; Lemon, S. J.; Truhlar, D. G.; Mead, C. A. *J. Chem. Phys.* **1985**, *82*, 5597.
(33) Press, W. H.; Flannery, B. P.; Teukolsky, S. A.; Vetterling, W. T. *Numerical Recipes;* Cambridge University Press: Cambridge, 1988; pp 420–435.
(34) Sorge, K. L.; Gibson, D. A.; Carter, E. A. Work in progress.

JP9433517